Optical model for light distribution during transscleral cyclophotocoagulation

Babak Nemati, Andrew Dunn, Ashley J. Welch, and H. Grady Rylander III

Transscleral cyclophotocoagulation (TSCPC) is currently performed clinically as an effective treatment for end-stage glaucoma. We develop a theoretical model for the analysis of optical attenuation phenomena during TSCPC as a basis for selection of an optimal wavelength. A multilayered Monte Carlo model was developed to calculate the fluence and the rate of heat generation in each tissue layer for the wavelengths of Nd:YAG, diode, ruby, krypton yellow, and argon lasers. Of the five wavelengths under study, our theoretical results suggest that the diode laser wavelength offers the best penetration through the conjunctiva, sclera, and ciliary muscle and highest absorption within the ciliary pigment epithelium.

OCIS codes: 160.4760, 290.0290, 300.1030.

1. Introduction

A large number of studies in the past few years have supported the use of transscleral cyclophotocoagulation (TSCPC) as a treatment for advanced glaucoma. TSCPC is a cyclodestructive procedure that is used to inhibit the production of aqueous humor by inducing coagulation necrosis in the ciliary body of the eye. The procedure involves the delivery of light, usually with a contact probe, through the superficial layers of conjunctiva and sclera to the ciliary body.

Historically, a number of different methods have been developed to ablate the ciliary processes, dating as far back as the early 1930's[1] and ranging from diathermy[1,2] to beta irradiation,[3] cyclocryotherapy,[4] and finally cyclophotocoagulation.[5] Beckman and Waeltermann[6] pioneered the transscleral irradiation of the ciliary body in patients with intractable glaucoma using the ruby laser as their light source. In 1984, Beckman and Waeltermann[6] reported a ten-year follow up on this study, with an 86% success rate for aphakic open-angle glaucoma. The limited availability of ruby lasers, however, leads to the continued use of cyclocryotherapy as the most common treatment for patients with intractable glaucoma.[7]

More recently, a number of studies have suggested the use of Nd:YAG laser for TSCPC.[8,9] Others have suggested the use of diode lasers (790–850 nm) for this treatment modality.[10] Both of these laser sources are currently in clinical use.

In spite of the large number of case studies that have been reported on the use of TSCPC, the choice of lasers and exposure parameters have been based largely on a clinical comparison of results with various lasers rather than a clear understanding of the treatment mechanism, the optical and thermal properties of tissue, or a sound theoretical model. Vogel *et al.*[11] were the first to carry out a measurement of the optical properties of human sclera in an attempt to investigate effective transscleral delivery of light for TSCPC. Using a standard integrating sphere method, the authors determined the optical properties of the sclera for five different wavelengths, including those of the argon (514-nm), diode (804-nm), and the Nd:YAG (1064-nm) lasers. Their results suggested that the near-infrared (NIR) lasers should prove to be more efficacious for the desired therapeutic end points of TSCPC.

In this study we aim to further the current knowledge of the underlying treatment mechanism for TSCPC by using the optical properties of the three layers involved in this procedure (i.e., conjunctiva, sclera, and the ciliary body) to model the distribution of light in these tissue layers. Using this model, we determined the depth and radially resolved fluence rate—and rate of heat deposition—in the multilay-

When this research was undertaken all of the authors were with the Medical Optics Laboratory, Biomedical Engineering Program, ENS 610, University of Texas, Austin, Texas 78712. B. Nemati is currently with Ethicon, Inc., P.O. Box 151, Somerville, New Jersey 08876-0151.

Received 19 May 1997; revised manuscript received 29 September 1997.

0003-6935/98/040764-08$10.00/0

ered tissue structure involved in TSCPC during laser irradiation with the five lasers, which have historically been used to carry out this procedure. This model can serve as a convenient and flexible tool for the characterization of the optical events during TSCPC, comparison of the utility of different laser sources for this procedure, prediction of appropriate dosimetry for each source, and design of an appropriate delivery system.

Previously measured optical properties of rabbit conjunctiva, sclera, and ciliary body[12] are used in a multilayered model for the tissue layers affected by TSCPC. The Monte Carlo method is used to estimate the fluence and the rate of heat generation in the respective tissue layers for the five different wavelengths that have been proposed by various investigators for TSCPC. The software for the Monte Carlo simulation was developed at the University of Texas at Austin.

2. Methods

A. Monte Carlo

The Monte Carlo method is a stochastic model that has been used to simulate problems that can be readily characterized by radiative transport theory (e.g., light propagation in biological media). The method consists of a detailed bookkeeping of the scattering and absorption experiences of each individual photon for a large number of photons as they propagate through a medium.

B. Algorithm

The Monte Carlo program continuously scatters photons as they propagate through a medium until they are absorbed by a chromophore, reflected from, or transmitted through, the medium. The tissue is assumed to be infinitely wide and is characterized by its (a) thickness t (centimeters), (b) refractive index n, (c) absorption coefficient μ_a (inverse centimeters), (d) scattering coefficient μ_s (inverse centimeters), and (e) anisotropy factor g. Photons are launched normal to the air–tissue interface and distributed along a radial line of width equal to the beam radius (300 μm). The physical quantities of interest that are estimated with the Monte Carlo simulation are the reflectance R, transmittance T, fluence rate $\phi(x, y, z)$ (watts per square centimeter), and photon absorption energy density (or rate of heat generation) $A(x, y, z)$ (watts per cubic centimeter).

The path of each photon in the medium is characterized by steps of randomly varying lengths and an angle of deflection from the previous scattering site.[13] The step sizes and the angles are sampled from their respective probability distributions. Upon scattering, the directional cosines for the deflection angle cos θ are determined by the Henyey–Greenstein scattering function, which provides a good analytical representation of single scattering in tissue.[14]

The Monte Carlo simulation used in this study incorporates a variance reduction technique whereby a packet of photons, representing many photons, is propagated simultaneously through a particular path within the medium. Each photon packet starts with an assigned weight W that is set equal to 1. Photons can either be terminated by reflection or transmission out of the tissue or absorbed within the medium. To ensure conservation of energy, and to avoid a bias in the distribution of photon deposition, a random termination technique known as the roulette is used. When the weight of a photon packet is reduced below a threshold value W_{th} (e.g., $W_{\text{th}} = 0.0001$), the roulette gives the photon bundle one chance in m (e.g., $m = 10$) of survival, with a weight of mW. Once the photon packet is terminated, its weight is set to zero, and this interaction marks the end of the photon's propagation within the medium. Given a pseudo-random number ξ, the roulette criterion for survival can be summarized as

$$W = \begin{cases} mW & \text{if } \xi \le 1/m \\ 0 & \text{if } \xi > 1/m \end{cases}. \tag{1}$$

When the photon packet is fully absorbed (terminated), a new photon packet is launched into the tissue and the same recordkeeping procedure is followed.

C. Multilayered Model for TSCPC

To apply the Monte Carlo simulation to the particular tissue geometry involved in transscleral irradiation of the ciliary body, we developed a four-layered model of the tissues adjacent to the corneo-scleral limbus of the eye. These layers, as illustrated schematically in Fig. 1, are (a) the conjunctiva and the Tenon's capsule, (b) the sclera, (c) the ciliary muscle, and (d) the ciliary pigment epithelium (CPE). The anterior interface is with air ($n = 1.00$) and the posterior interface is with the vitreous humor of the eye ($n = 1.34$). A slab geometry, as required by the Monte Carlo simulation, is used for all layers, and the tissues are assumed to be of infinite lateral extent, which is a justified assumption for the wavelengths under study (514–1064 nm).

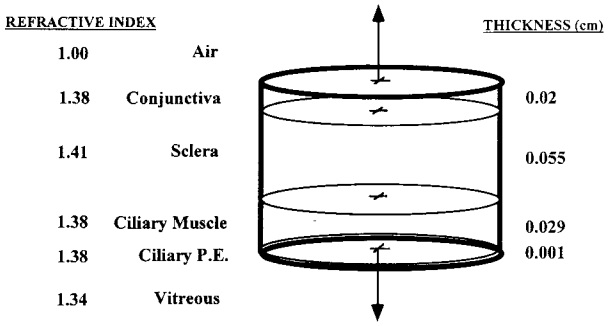

Fig. 1. Multilayered tissue structure involved in TSCPC.

We obtained optical properties using a UV–vis–NIR spectrophotometer, as reported previously.[12] We performed a biopsy of an intact rabbit eye, excising separate specimens of conjunctiva, sclera, and ciliary body. For the Monte Carlo simulation, the anisotropy factor g was assumed to be 0.9.

We calculated the optical properties of the CPE by

Table 1. Optical Properties of Rabbit Model as used in the Monte Carlo Simulation[a]

Laser Source	CPE		Ciliary Muscle		Sclera		Conjunctiva	
	μ_a	μ_s	μ_a	μ_s	μ_a	μ_s	μ_a	μ_s
Argon (~500 nm)	693	0	30	385.5	2.8	684	1.2	114
Krypton (~550 nm)	595	0	29.6	400	2.5	612	1.8	108
Ruby (~700 nm)	429	0	22.8	480.4	1.7	410	0.4	71
Diode (~850 nm)	282	0	13	536	1.3	245	0.5	64
Nd:YAG (~1050 nm)	94	0	4.75	516.1	1.8	164	0.3	52
			μ_a (cm^{-1})		μ_s (cm^{-1})			

[a]See Ref. 11. Note that the optical properties shown for CPE are those measured for the rabbit retinal pigment epithelium. Anisotropy factor g was assumed to be 0.9.

assuming that (a) absorption is the dominant attenuation process in the pigmented epithelium (i.e., μ_s is negligible as compared with μ_a and is therefore set to zero), and (b) at the argon laser wavelength (approximately 500 nm) 50% of the light is transmitted.[15] Using Beer's law we calculated the absorption coefficient for a 10-μm layer of CPE (as measured from histology specimens[16]), and we calculated the absorption coefficient for the remaining wavelengths using the line shape for the absorption coefficient of the retinal pigment epithelium, as reported previously by other investigators.[15,17]

To calculate the ciliary body optical properties, we measured diffuse transmission through and diffuse reflectance from the ciliary body. If this structure is thought of as a double layer, comprised of a ciliary muscle layer and a CPE layer, the diffuse transmission measured through the entire structure can be considered as the amount of light transmitted through the posterior interface of the CPE. Because we assumed that light attenuation within this layer is dominated by absorption and that it is governed by Beer's law, we calculated light that was incident on the anterior interface of the CPE layer. This value also represents the diffuse transmission through the ciliary muscle layer. Given this value for diffuse transmission through the ciliary muscle, and the reflectance value measured for the entire ciliary body from the anterior interface of the ciliary muscle, we then calculated the optical properties of ciliary muscle using an inverse adding–doubling algorithm. Table 1 lists the optical properties that we used in constructing the multilayered tissue model.

Calibration data for the integrating sphere measurements were provided by the manufacturer in increments of 50 nm. As such, in the given model we used approximate wavelengths for each laser source. The optical properties for the following five wavelengths were used to run the Monte Carlo simulation: (a) $\lambda = 500$ nm, approximating the dominant emission peak of argon laser at 514 nm; (b) $\lambda = 550$ nm, approximating the krypton yellow laser wavelength of 568 nm; (c) $\lambda = 700$ nm, approximating the dominant ruby laser wavelength of 693 nm; (d) $\lambda = 850$ nm for a typical GaAs semiconductor diode laser; and (e) $\lambda = 1050$ nm, approximating the Nd:YAG laser wavelength of 1064 nm.

We validated our simulation results against results obtained from the published Monte Carlo (MCML) code of Wang and Jacques.[18] Our results are in close agreement to the results obtained from the published MCML code.

D. Simulation Parameters

Tissue thicknesses for the conjunctiva and the sclera were determined from an average of measurements on a group of five rabbits. The values used for each thickness are shown in Fig. 1.

Even though the simulation is over a continuous space, the location of absorbed light is expressed in terms of a cylindrical r–z structure. The width of each grid element along the z direction dz was chosen to be 5 μm, or half the width of the thinnest layer (the CPE) that was assumed to be approximately 10 μm in thickness (as verified by histology slides). We then calculated the total number of grid elements along the z direction (210 elements) by dividing the total thickness of the four-layered structure by dz.

The contact fiber-optic probe was assumed to have a diameter of 600 μm, and because the fiber was in contact with the tissue, a flat beam profile was chosen for the simulation. The 600-μm diameter of the fiber is considered the spot size of the incident beam on the conjunctival surface. To obtain a reasonable resolution in the r direction, dr was chosen to be 30 μm, and the total radial length for this simulation was set at 750 μm, giving a total number of 25 grid elements in the r direction.

The simulated response of the tissue to a flat-top beam of 300-μm radius, whose total power was fixed at 1 W, was obtained with a total of 500,000 photons for the five wavelengths indicated above. The irradiance at the anterior surface of the multilayered structure simulated was 354 W/cm.[2]

3. Results

The Monte Carlo simulation was used to calculate the fluence rate (watts per square centimeter) and rate of heat generation (watts per cubic centimeter) within and transmittance through the multilayered tissue structure described above. For discussion purposes, in the remainder of this paper, we limit all comparisons to the Nd:YAG, diode, and argon laser wavelengths. The results from the krypton yellow and ruby laser wavelengths typically fall between those obtained for the argon and diode wavelengths and have been omitted here to avoid cluttering in the graphs and the corresponding discussion. Reflectance, transmittance, and absorbance for all wavelengths are summarized in Table 2.

A. Distribution Contours of Internal Fluence Rate

The contour plot of the fluence rate for the Nd:YAG and argon laser wavelengths are shown in Figs. 2 and 3, respectively. In TSCPC, one of the desired features of the transscleral-delivered light is a narrow angular distribution to minimize photocoagulative ef-

Table 2. Calculated Fraction of Reflection, Absorption, and Transmission for the Multilayered Tissue Structure for the Five Wavelengths of 500, 550, 700, 850, and 1050 nm

Laser	Wavelength (nm)	Specular Reflection	Diffuse Reflection	Absorption	Transmission
Argon	500	0.0255	0.343	0.619	0.011
Krypton	550	0.0255	0.318	0.642	0.014
Ruby	700	0.0255	0.325	0.614	0.036
Diode	850	0.0255	0.273	0.607	0.095
Nd:YAG	1050	0.0255	0.235	0.507	0.233

fects to the surrounding tissues. A comparison of Figs. 2 and 3 shows the advantages of the Nd:YAG laser wavelength over the argon laser wavelength in maintaining lower radial spread of the delivered light to the ciliary body. The contours of Fig. 2 also demonstrate the more penetrating nature of the Nd:YAG laser light.

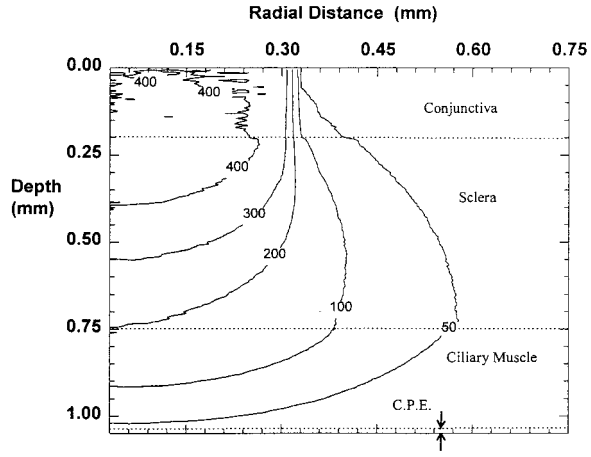

Fig. 2. Fluence rate (watts per square centimeter) as a function of radial distance r (centimeters) and depth z (centimeters) for λ = 1050 nm (approximating the dominant Nd:YAG laser wavelength of 1064 nm).

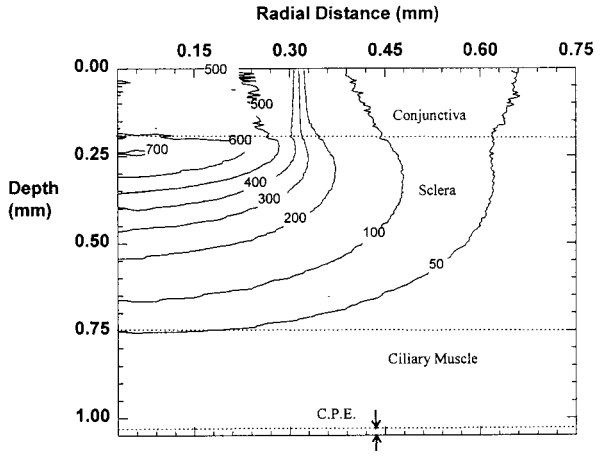

Fig. 3. Fluence rate (watts per square centimeter) as a function of radial distance r (centimeters) and depth z (centimeters) for λ = 500 nm (approximating the dominant argon laser wavelength of 514 nm).

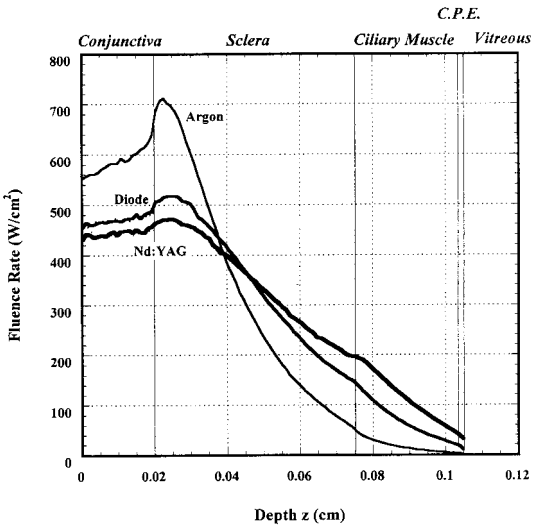

Fig. 4. Fluence rate (watts per square centimeter) along the z axis directly under the beam at r = 0.0015 cm for the wavelengths of (a) 500 nm (approximating the dominant argon laser wavelength of 514 nm), (b) 850 nm (GaAs diode laser wavelength), and (c) 1050 nm (approximating the Nd:YAG laser wavelength of 1064 nm) for a flat incident beam profile (radius, 300 μm; total power, 1 W).

B. Depth-Resolved Internal Fluence Rate

The depth-dependent changes in fluence rate for the three wavelengths of argon, diode, and Nd:YAG lasers are compared in Fig. 4. Because of the high scattering for the argon laser wavelength, the fluence for argon laser quickly peaks at the anterior layers of the sclera (as high as approximately 715 W/cm^2), after which the fluence rapidly diminishes almost completely by the time light reaches the CPE. Laser light of the more penetrating wavelengths of diode and Nd:YAG lasers, however, achieve slightly lower fluence rates within the sclera (approximately 520 and 470 W/cm^2, respectively), and drop to 18 and 37 W/cm^2, respectively, by the time light reaches the pigment epithelium.

Also note that the internal fluence rate within the tissue is significantly higher than the irradiance at the conjunctival surface (354 W/cm^2 for the incident 1 W and a beam radius of 300 μm). For example, for the argon laser wavelength, the peak internal fluence rate at the anterior layers of the sclera is 31% higher than the irradiance just below the air–tissue interface. This phenomenon is to be expected, since the large backscattered component for this wavelength augments the internal fluence.

Another point of interest is the relatively low fluence rate at the CPE. Even in the case of the most penetrating wavelength, the Nd:YAG laser wavelength, the fluence rate in the CPE is approximately 37 W/cm^2, which is approximately 8% of the fluence in the anterior layers of the sclera.

C. Depth-Resolved Rate of Heat Generation

The depth-resolved rate of heat generation (heat source) directly under the beam ($r = 0.0015$ cm) for the three wavelengths of argon, diode, and Nd:YAG lasers is shown in Fig. 5. As expected, the rate of heat generation within the sclera is the highest for the argon laser wavelength, reaching 2000 W/cm^3. Within the stroma of the ciliary muscle, however, the highest rate of heat generation is associated with the diode laser wavelength at the suprachoroidal space. At this depth and directly under the beam, the rate of heat generation for the diode laser wavelength (1850 W/cm^3) is approximately 30% higher than that for the argon (1410 W/cm^3) and 100% higher than the rate of heat generation for the Nd:YAG (930-J/cm^3) laser wavelengths. Within the CPE, because of the high absorption coefficient of this layer, the rate of heat generation is high for all wavelengths, but highest for the diode laser wavelength (3970 W/cm^3), which is 21% higher than the rate of heat generation for the Nd:YAG (3280 W/cm^3) and 132% higher than that calculated for the argon (1710-W/cm^3) laser wavelength.

Because the rate of heat generation for all three wavelengths is relatively high, given the appropriate exposure parameters, it is conceivable that all the wavelengths under study are capable of producing acute thermal damage to the CPE. It is likely, however, that such acute effects within the pigment epithelium are also accompanied by significant acute thermal damage to the entire multilayered structure, including the sclera and the ciliary stroma.

D. Transmittance, Reflectance, and Absorbance

The reflectance, absorbance, and transmittance of the light for the five laser wavelengths under study, through the entire multilayered tissue structure, are listed in Table 2. Because of the small tissue thicknesses for the rabbit model, the transmission of light into the vitreous is relatively high for all five wavelengths. In the human model, the sclera and the ciliary body are approximately twice as thick, and therefore the total transmission of laser light into the eye is expected to be significantly less than the values calculated for the rabbit model. Moreover, since the radiation is diffuse, other than potential patient discomfort, it is unlikely that this radiation would lead to any significant retinal damage.

4. Discussion

Among the first results that have been documented on the use of argon laser for TSCPC was the study reported by Peyman *et al*. in 1984 entitled "Histopathologic studies on transscleral Argon-Krypton photocoagulation with an exolaser probe".[19] In this study the authors examined the use of argon and krypton lasers for transscleral contact photocoagulation of the retina and the ciliary body in rabbits and found no significant difference in the energetic parameters needed for the two laser wavelengths to establish threshold coagulative lesions. Furthermore, the authors performed a 360° cyclophotocoagulation on rabbits and reported a sustained pressure-lowering effect for only 4 to 7 days. The limited success of this study in lowering rabbit intraocular pressure (IOP) is understandable, however, because all the transscleral lesions in their study were found to be posterior to the ciliary processes.

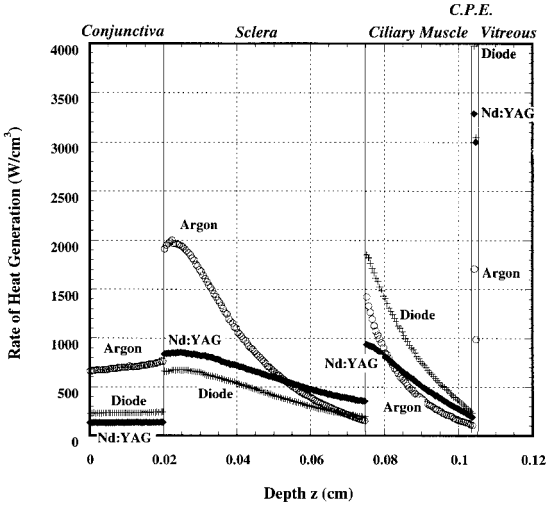

Fig. 5. Rate of heat generation (watts per cubic centimeter) directly under the beam as a function of depth z (centimeters) for wavelengths: (a) 500 nm (approximating the dominant argon laser wavelength of 514 nm), (b) 850 nm (GaAs diode laser wavelength), and (c) 1050 nm (approximating the Nd:YAG laser wavelength of 1064 nm) for a flat incident beam profile (beam radius, 0.03 cm; total power, 1 W). The radial distance was held fixed at 0.0015 cm.

The experience of Peyman *et al*. is representative of a large number of studies that were carried out prior to the 1990's when sufficient information on proper probe placement or appropriate dosimetry for TSCPC was not yet available. It appears that the clinical community, however, abandoned alternative wavelengths to the Nd:YAG laser wavelength as viable laser sources for cyclophotocoagulation largely based on these preliminary studies.

In 1984 Beckman and Waeltermann reported a 10-year follow-up study[6] on 241 human eyes that were treated with transscleral ruby cyclophotocoagulation with an overall success rate (defined as a sustained IOP between 5 and 22 mm Hg) of 62% (150 of 241 eyes). The success rate for this study varied from 86% for aphakic open-angle glaucoma (32 of 37 eyes) to 53% for neovascular glaucoma (72 of 135 eyes). This laser source was also abandoned, not because of poor clinical results, but mainly because of the unavailability of ruby lasers and problems associated with the technology itself.

More recently, Immonen *et al*.[20] have reported the clinical use of krypton laser for transscleral contact cyclophotocoagulation in 62 eyes of 57 patients refractory to alternative surgical treatments. In comparison with Peyman *et al*.'s preliminary study in 1984 (cited above), the protocol used in Immonen *et al*.'s recent study is much more accurate in targeting of the ciliary processes (lesions were placed at an

average distance of 1.9-mm posterior to the limbus) and in the dosimetry used. Given these improvements, Immonen *et al*. had an 82% success rate after 6 months in preserving vision and lowered the baseline mean IOP of 34.8 ± 11.0 mm Hg to a mean level of 20.9 ± 9.1 mm Hg in the same time span. Furthermore, they reported no clinical signs of scleral injury or loss of vision (common cyclodestructive complications) in the pool of patients treated.

Such positive results on the use of visible wavelengths for cyclophotocoagulation merit a closer look at these laser sources that are readily available in most ophthalmic clinics. The simulation that we present in this paper is intended to set a framework for a comparative analysis of the optical and thermal events resulting from TSCPC using the five wavelengths that have been used for this clinical procedure. The Monte Carlo simulation provides a convenient and flexible tool for the theoretical analysis of light distribution and the rate of heat generation within the multilayered tissue structure involved in TSCPC for different wavelengths of incident laser radiation.

Based on the optical properties of the conjunctiva, sclera, and the ciliary body (Table 1), we expect the NIR wavelengths of Nd:YAG and diode lasers to be more penetrating than the wavelengths of the argon, krypton, and ruby lasers. Figure 4 confirms this expectation, which is consistent with earlier histopathologic studies of human and rabbit sclera, after TSCPC, that demonstrated minimal changes to the sclera as a result of diode or Nd:YAG laser irradiation.[10,21] Figure 4 further shows that, for all wavelengths under study, the fluence drops significantly through the sclera and the ciliary muscle, and, by the time light traverses these two layers, very low fluence (of the order of 20 W/cm^2) is delivered to the CPE. The rate of heat generation, however, is affected by the fluence rate as well as the absorption coefficient that is high for the CPE for all the wavelengths under study.

When comparing the rate of heat generation, Fig. 5 shows that, in spite of the higher fluences that are due to the Nd:YAG laser irradiation, the absorption energy density for the diode laser is the highest of the five wavelengths in the ciliary muscle and the CPE. The argon laser light is absorbed substantially within the sclera and the ciliary muscle, and, as a result, the rate of heat generation within the target tissue (the pigment epithelium) is much lower for this wavelength. These theoretical results predict that the acute thermal damage to the CPE is highest for the diode laser wavelength. However, because the rate of heat generation in the ciliary muscle is also the highest for this wavelength, it is likely that the pain associated with use of this laser wavelength is also highest in comparison with the other five wavelengths under investigation.

A number of investigators have confirmed the above theoretical predictions by examining the acute response of the ciliary body to diode laser TSCPC. Hennis and Stewart carried out a histologic evaluation of human cadaver eyes that had undergone TSCPC using diode laser sources (wavelengths ranging from 780 to 830 nm). Their investigation revealed that transscleral diode laser irradiation of the peri limbal region led to extensive tissue shrinkage, marked fragmentation, edema, and detachment of the epithelium.[10]

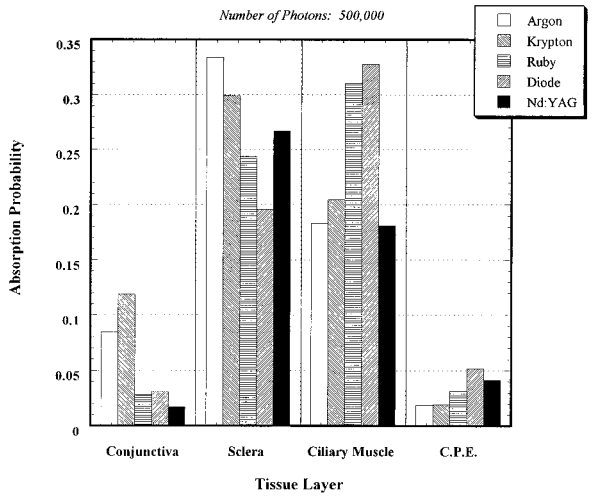

Fig. 6. Probability of photon absorption for each layer of the model for Nd:YAG, diode, ruby, krypton, and argon laser wavelengths.

Schuman *et al*. reported a comparative histopathologic evaluation of rabbit eyes that had undergone diode laser and Nd:YAG laser TSCPC.[22] The authors concluded, however, that grossly, the ciliary destruction resulting from both of these laser sources are comparable. To the extent that the tissue coagulative response is affected by dosimetry, probe placement, and delivery mode, it is conceivable that, under identical treatment conditions, the difference in the extent of ciliary destruction between diode and Nd:YAG laser sources that is predicted by our model presented here can be demonstrated clinically.

The data presented in Fig. 5 suggest that, even for the most penetrating wavelength under study (the Nd:YAG laser wavelength), the absorption energy density directly under the beam is sufficiently high to produce acute thermal damage to all layers, including the ciliary muscle. As such, it appears that a full-thickness acute thermal damage results from TSCPC when all the wavelengths under study are used. Figure 6 illustrates the probability of photon absorption for each layer of the model, for the five laser wavelengths, and clearly shows significant absorption for all wavelengths in the sclera and ciliary muscle and less-pronounced absorption in the conjunctiva and CPE.

We experimentally observed the full-thickness nature of the thermal insult that is due to TSCPC using Nd:YAG, diode, and argon laser wavelengths.[16] A recent study by Ferry *et al*. provided a detailed histopathologic examination of the nature of the lesions produced as a result of Nd:YAG laser TSCPC.[23] The

authors reported severe degeneration of the stroma and ciliary muscle, and that in all cases under study, the ciliary muscle was severely damaged.

These findings are consistent with the prediction of our model. Given the relatively high rate of heat generation within the anterior layers of the ciliary muscle, it is likely that, for all the wavelengths under investigation, the ciliary stroma suffers acute thermal damage during TSCPC. This prediction suggests that the mechanism of IOP lowering could be related to both acute thermal necrosis of the CPE and secondary necrosis of this structure that is due to thermolysis of the supplying vasculature in the ciliary stroma. Because it appears that all the wavelengths under study, including the penetrating Nd:YAG laser wavelength, induce some level of thermal damage to the vasculature within the ciliary stroma, a certain level of such acute thermal damage may be tolerable and may serve a role in reducing intraocular pressure.

In considering the visible wavelength lasers for TSCPC, the results shown in Figs. 4 through 6 clearly suggest that the only viable approach for use of these wavelengths for TSCPC is through reducing their attenuation within the sclera. A number of investigators have demonstrated the benefits of direct mechanical pressure in increasing scleral transparency.[11] In our laboratories, we also explored the use of topical chemical agents to achieve transient scleral transparency and experimented with temperature-dependent dynamic changes in scleral transparency (unpublished results). Based on the present model, it appears that, whereas visible wavelength TSCPC may achieve comparable IOP lowering effects as NIR laser wavelengths, one or several of the above approaches need to be adopted to minimize thermal damage to the sclera and to reduce damage to the ciliary muscle. Kivela *et al*. recently reported results from a clinically successful treatment with contact krypton laser TSCPC in which the authors had the opportunity to perform a histopathologic and immunohistochemical autopsy evaluation of the treated eye.[24] Their study demonstrated that the effect of the transscleral krypton laser irradiation left the sclera and zonules intact while causing significant disruption of the ciliary processes.

In the present study, the optical properties used to construct the model were measured from *in vitro* samples that were void of their blood content. We expect that the presence of blood *in vivo* will have a significant effect on the optical and thermal behavior of these tissues (particularly the conjunctiva and the ciliary muscle) in response to transscleral irradiation with the five wavelengths under study. When more-refined techniques for measurement of optical properties *in vivo* become available, it will be possible to use the model presented here to arrive at a more accurate analysis of the optical and thermal events involved in TSCPC. Furthermore, we have not considered the impact of dynamic changes in the optical properties of the tissue involved on the delivery of light to the CPE. It is conceivable that the coagulative necrosis within the ciliary stroma may substantially attenuate the incident radiation and further reduce the fluence levels at the CPE. A confirmation of this conjecture requires a thorough analysis of the dynamic optical properties of the tissues involved in cyclophotocoagulation, which will need to be investigated in future studies.

5. Conclusions

The Monte Carlo model for the analysis of light distribution in tissue provides a convenient and flexible method for exploring a variety of optical phenomena associated with TSCPC, which are difficult to measure experimentally. With the optical properties measured previously,[11] the present study applies the Monte Carlo method for the multilayered tissue structure involved in cyclophotocoagulation for the five wavelengths of argon, krypton, ruby, diode, and Nd:YAG lasers. The Monte Carlo simulation calculates the distribution of fluence and absorption energy density within the medium under study. Our results suggest that, whereas the Nd:YAG laser wavelength achieves the highest fluence in the CPE, the highest rate of heat generation within this tissue layer can be achieved with the diode laser wavelength. It is likely that all wavelengths under study lead to a full-thickness thermal insult to the multilayered tissue structure involved in TSCPC, and although visible wavelength TSCPC may achieve comparable IOP lowering effects as the NIR wavelengths, additional measures need to be taken to minimize thermal damage to the sclera.

This research was supported in part by the Office of Naval Research (grant N00014-91-J-1564) and the U.S. Department of Energy (DE-FGO3-95ER611971).

References

1. H. Weve, "Die Zyklodiatermie das Corpus Ciliare bei Glaukom," Zenterlabl Ophthalmol. **97,** 562–569 (1933).
2. D. S. Walton and W. M. Grant, "Penetrating cyclodiathermy for filtration," Arch. Ophthalmol. **83,** 47–48 (1970).
3. G. M. Haik, L. A. Breffeilh, and A. Barbar, "Beta irradiation as a possible therapeutic agent in glaucoma: an experimental study with the report of a clinical case," Am. J. Ophthalmol. **31,** 945–952 (1948).
4. F. M. Polack and A. de Roetth, "Effect of freezing on the ciliary body (cyclocryotherapy)," Invest. Ophthalmol. **3,** 164 (1964).
5. P. F. Lee and O. Pomerantzeff, "Transpupillary cyclophotocoagulation of rabbit eyes: an experimental approach to glaucoma surgery," Am. J. Ophthalmol. **71,** 911–920 (1971).
6. H. Beckman and J. Waeltermann, "Transscleral ruby laser cyclophotocoagulation," Am. J. Ophthalmol. **98,** 788–795 (1984).
7. J. S. Schuman and C. A. Puliafito, "Laser cyclophotocoagulation," Int. Ophthalmol. Clin. **30,** 111–119 (1990).
8. J. S. Schuman, A. R. Bellows, B. J. Shingleton, M. A. Latina, R. R. Allingham, C. D. Belcher, and C. A. Puliafito, "Contact transscleral Nd:YAG laser cyclophotocoagulation. Midterm results," Ophthalmology **99,** 1089–1094 (1992).
9. M. M. Wright, A. L. Grajewski, and W. J. Feuer, "Nd:YAG cyclophotocoagulation: outcome of treatment for uncontrolled glaucoma," Ophthalmic Surg. **22,** 279–283 (1991).
10. H. L. Hennis and W. C. Stewart, "Semiconductor diode laser

transscleral cyclophotocoagulation in patients with glaucoma," Am. J. Ophthalmol. **113,** 81–85 (1992).
11. A. Vogel, C. Dlugos, R. Nuffer, and R. Birngruber, "Optical properties of human sclera, and their consequences for transscleral laser applications," Lasers Surg. Med. **11,** 331–340 (1991).
12. B. Nemati, H. G. Rylander III, and A. J. Welch, "Optical properties of conjunctiva, sclera, and ciliary body and their consequences for transscleral cyclophotocoagulation," Appl. Opt. **35,** 3321–3327 (1996).
13. M. Keijzer, S. L. Jacques, S. A. Prahl, and A. J. Welch, "Light distribution in artery tissue: Monte Carlo simulations for finite diameter laser beams," Lasers Surg. Med. **9,** 148–154 (1989).
14. S. L. Jacques, C. A. Alter, and S. A. Prahl, "Angular dependence of HeNe laser light scattering by human dermis," Lasers Life Sci. **1,** 309–333 (1987).
15. W. J. Geeraets, R. C. Williams, G. Chan, W. T. Ham, Jr., D. P. Guerry III, and F. H. Schmidt, "The relative absorption of thermal energy in retina and choroid," Invest. Ophthalmol. **1,** 340–347 (1962).
16. B. Nemati, "Transscleral argon cyclophotocoagulation: a preclinical feasibility study," Ph.D. dissertation (University of Texas, Austin, Tex., 1995).
17. E. B. Boettner and J. R. Wolter, "Transmission of the ocular media," Invest. Ophthalmol. **1,** 776–783 (1962).
18. L. Wang and S. Jacques, "Monte Carlo modeling of light transport in tissues," in *Optical-Thermal Response of Laser-Irradiated Tissue*, A. J. Welch and M. J. C. van Gemert, eds. (Plenum, New York, 1995), pp. 73–100.
19. G. A. Peyman, M. D. Conway, M. Raichand, and J. Lin, "Histopathologic studies on transscleral argon-krypton photocoagulation with an exolaser probe," Ophthalmic Surg. **15,** 496–501 (1984).
20. I. Immonen, P. Puska, and C. Raitta, "Transscleral contact krypton laser cyclophotocoagulation for treatment of glaucoma," Ophthalmology **101,** 876–882 (1994).
21. C. Hampton and M. B. Shields, "Transscleral neodymium:YAG cyclophotocoagulation: a histologic study of human autopsy eyes," Arch. Ophthalmol. **106,** 1121–1123 (1988).
22. J. S. Schuman, J. J. Jacobson, C. A. Puliafito, R. J. Noecker, and W. T. Reidy, "Experimental use of semiconductor diode laser in contact transscleral cyclophotocoagulation in rabbits," Arch. Ophthalmol. **108,** 1152–1157 (1990).
23. A. P. Ferry, M. H. King, and D. W. Richards, "Histopathologic observations of human eyes following neodymium:YAG laser cyclophotocoagulation for glaucoma," Trans. Am. Ophthalmol. Soc. **93,** 315–331 (1995).
24. T. Kivela, P. Puska, C. Raitta, I. Immonen, and A. Tarkkanen, "Clinically successful contact transscleral krypton laser cyclophotocoagulation," Arch. Ophthalmol. **113,** 1447–1453 (1995).